*Journal of Engineering Mathematics* **49:** 359–372, 2004.


# Self-propagating free-radical binary frontal polymerization

M.F. PERRY and V.A. VOLPERT
*Department of Engineering Sciences and Applied Mathematics, Northwestern University, Evanston, IL 60208-3125, U.S.A.*

Received 15 May 2003; accepted in revised form 2 February 2004

**Abstract.** The first mathematical model for free-radical binary frontal polymerization (BFP), is presented. The model describes the following experimental situation. A test tube is filled with a mixture of two monomers and an initiator. When the temperature at the top of the tube is increased a self-sustained polymerization wave which propagates along the axis of the tube is formed. Two different polymer species are synthesized in the wave. Such one-dimensional polymerization waves are studied. Approximate analytical solutions are derived and compared to numerical solutions. The effect of various parameters of the model on the front velocity and temperature is discussed.

**Key words:** binary free-radical polymerization, frontal polymerization, modeling

## 1. Introduction

Frontal polymerization (FP) is a method of manufacturing polymer via a self-propagating reaction wave. The reaction wave is formed when the temperature is locally increased to the reactant-dependent ignition temperature. This wave propagates through the medium converting the initial reactants into polymer product. Chemical conversion occurs in a narrow region of the wave, called the reaction front. The front separates the medium into two distinct regions, reactants ahead of the front and product behind the front. The physical state of these regions depends upon the reactants and the conditions of the experiment, but typically the monomers are liquid and the polymer is either a solid or a very viscous liquid.

Front propagation is due to the exothermicity of the polymerization reactions and the diffusion of heat. The chemical mechanism for FP is usually free-radical polymerization. However, FP has also been demonstrated in polymerization processes with different chemical kinetics such as epoxy curing [1] and ring-opening metathesis [2].

Free-radical frontal polymerization falls into the classification of chain polymerization. As the name indicates, the polymer product is formed by successive linking of monomer molecules in a chain-like fashion. Homopolymerization refers to systems that contain one type of monomer; binary and copolymerization are systems that contain two (or possibly more in the case of copolymerization) types of monomers. Binary polymer chains grow by successively adding the same type of monomer radical to the end of the chain and are analogous to forming two homopolymers in the same system. Copolymers contain units of both monomers in each copolymer molecule [3]. Binary polymerization and copolymerization are effective methods for creating polymers with specific qualities like an increase in strength, more flexibility, oil and grease resistance, or better impact resistance [4]. Simultaneous inter-penetrating polymer networks (IPNs) were demonstrated with binary frontal polymerization using a combination of an epoxy monomer, which forms a step polymer, and a free-radical monomer [5].

The history of frontal polymerization begins in 1972 with the work of Chechilo *et al.* [6]. They developed FP as the polymer analog to self-propagating high-temperature synthesis (SHS) [7], a combustion process used to make ceramics and intermetallic compounds. Their research on methyl-methacrylate frontal polymerization showed that front velocity and polymer composition are influenced by initiator species, initiator concentration and pressure change [6, 8–10]. Subsequent experimental work [11–14] demonstrated free-radical frontal polymerization for a variety of monomers. Most of these experiments used liquid neat monomers. However, FP has also been observed in systems with solid monomers [15, 16], in dispersions [17], and in solutions [18]. Along with demonstrating the feasibility of FP with particular monomers, experiments have also studied which conditions most affect the process and how to produced polymers with specific desired properties, *e.g.* functionally gradient polymeric materials [19], temperature-sensitive hydrogels [20], thermochromic composites [21, 22], and conductive composites [23].

Mathematical models of frontal homopolymerization and copolymerization have been successfully developed. The solutions of these models have been both numerical [24–27] and analytical [24, 27]. In these works, theoretical results are compared to experimental results to demonstrate the reliability of the models.

Stability of the propagating front has also been investigated. Experimental studies have examined convective instabilities [28, 29] and the nonlinear dynamics of the polymerization wave [30–33]. Theoretical studies include linear stability analyses [34, 35] and weakly nonlinear analysis of FP [36].

In this paper we present the first mathematical model which describes the following free-radical binary frontal polymerization (BFP) experiment. A test tube is filled with a mixture of two monomers and an initiator. Then, the temperature at the top of the tube is increased, forming a self-sustained polymerization wave that propagates along the axis of the tube. Our model describes such one-dimensional polymerization waves. We derive approximate analytic solutions to our equations and compare these results to numerical solutions. We also study how the various parameters of the model influence the front velocity and temperature.

## 2. Mathematical model

In this section, we outline the kinetic scheme of the reactions and present the mathematical model. As is typical with all chain polymerization, there are three steps – initiation, propagation and termination [3].

Initiation involves two reactions. In the first reaction the initiator ($I$) decomposes into two active radicals ($R$):

$$I \xrightarrow{k_d} 2R,$$

where $k_d$ is the rate constant for initiator decomposition. The second initiation reaction attaches the radical species to their respective monomers to form live monomer radicals $M^*_{j,1}$ ($j = 1, 2$)

$$R + M_1 \xrightarrow{k_{p1}} M^*_{1,1}, \quad R + M_2 \xrightarrow{k_{p2}} M^*_{2,1}. \tag{1}$$

The quantities $k_{p1}$ and $k_{p2}$ are the rate constants for these reactions.

The addition of monomer $M_1$ to $M^*_{1,n}$ (a monomer radical that consists of $n$ monomers $M_1$, $n = 1, 2, 3, \ldots$) and monomer $M_2$ to $M^*_{2,m}$ (a monomer radical that consists of $m$ monomers $M_2$, $m = 1, 2, 3, \ldots$) represents the propagation step

$$M^*_{1,n} + M_1 \xrightarrow{k_{p1}} M^*_{1,n+1}, \quad M^*_{2,m} + M_2 \xrightarrow{k_{p2}} M^*_{2,m+1}. \tag{2}$$

Note that the propagation rate constants $k_{p1}$ and $k_{p2}$ in (2) are taken to be the same as in (1) as discussed in [37]. Propagation forms live polymer chains. These chains continue to grow until two live polymer chains of the same type attach to each other to terminate the reaction

$$M^*_{1,n} + M^*_{1,m} \xrightarrow{k_{t1}} P_1, \quad M^*_{2,k} + M^*_{2,l} \xrightarrow{k_{t2}} P_2.$$

The rate constant for termination is represented by $k_{tj}$. Typically the terminated polymer chains are called dead polymer to signify that growth has ended.

From the mechanism described above, we generate the following mathematical model where the kinetic equations represent the mass balance of all of the species:

$$\frac{\mathrm{d}I}{\mathrm{d}t} = -k_d I, \tag{3a}$$

$$\frac{\mathrm{d}R}{\mathrm{d}t} = 2k_d I - k_{p1} R M_1 - k_{p2} R M_2, \tag{3b}$$

$$\frac{\mathrm{d}M_1}{\mathrm{d}t} = -k_{p1} R M_1 - k_{p1} M_1 M_1^*, \tag{3c}$$

$$\frac{\mathrm{d}M_2}{\mathrm{d}t} = -k_{p2} R M_2 - k_{p2} M_2 M_2^*, \tag{3d}$$

$$\frac{\mathrm{d}M_1^*}{\mathrm{d}t} = k_{p1} R M_1 - 2k_{t1} M_1^{*2}, \tag{3e}$$

$$\frac{\mathrm{d}M_2^*}{\mathrm{d}t} = k_{p2} R M_2 - 2k_{t2} M_2^{*2}. \tag{3f}$$

In these equations $t$ represents time, $I$ denotes initiator concentration, $R$ denotes the concentration of primary free radicals, $M_1$ and $M_2$ denote monomer concentrations, and $M_1^*$ and $M_2^*$ denote the concentration of live monomer radicals consisting of $M_1$ and $M_2$, respectively (we do not distinguish between monomer radicals of different lengths, and introduce $M_1^* = \sum_n M^*_{1,n}$, $M_2^* = \sum_m M^*_{2,m}$). All quantities of the form $k_\alpha$ (where $\alpha$ is $p1$, $p2$, $t1$ and so on), represent reaction rate constants, which, in fact, depend upon the temperature $T$ of the medium and are given by an Arrhenius relationship

$$k_\alpha = k_\alpha^0 \exp[-E_\alpha/(R_g T)].$$

Here $R_g$ is the gas constant, and $k_\alpha^0$ and $E_\alpha$ are the collision frequency factor and activation energy for the respective reaction rate constant.

Since the polymerization process is exothermic and the reaction rates depend upon temperature, we introduce an equation for temperature that accounts for thermal diffusion and heat release by the exothermic propagation reactions,

$$\frac{\partial T}{\partial t} = \kappa \nabla^2 T - q_1 \frac{\partial M_1}{\partial t} - q_2 \frac{\partial M_2}{\partial t}. \tag{4}$$

In this equation, $\nabla^2$ is the Laplacian with respect to the spatial variables $\xi = (\xi_1, \xi_2, \xi_3)$ ($\xi_1$ is the coordinate along the test tube axis), $\kappa$ is the thermal diffusivity of the mixture, and $q_1$ and $q_2$ represent the temperature increase due to the consumption of 1 mol/liter of $M_1$ and $M_2$, respectively. We assume that $\kappa$, $q_1$, and $q_2$ are constant.

We simplify this system of equations by introducing the steady-state assumption for radical concentration. The assertion is that after a transition period, the primary radical concentration and the monomer radical concentrations remain nearly constant. This has been justified for frontal polymerization in [37]. To implement this assumption we set the time derivatives in Equations (3b), (3e), and (3f) to zero, and solve the resulting system of algebraic equations for $R$, $M_1^*$, and $M_2^*$ to obtain

$$R = 2\rho\frac{k_d J^2}{k_{p1}M_1}, \quad M_1^* = \sqrt{\frac{k_d}{k_{t1}}}\sqrt{\rho}J \quad \text{and} \quad M_2^* = \sqrt{\frac{k_d}{k_{t2}}}\sqrt{1-\rho}J.$$

In the above equations

$$J = \sqrt{I}, \quad \rho = \frac{k_{p1}M_1}{k_{p1}M_1 + k_{p2}M_2} \equiv \frac{K_p M_1}{K_p M_1 + M_2},$$

where $K_p = k_{p1}/k_{p2}$.

If we substitute the approximations of $M_1^*$ and $M_2^*$ in Equations (3c) and (3d), neglect the $R$ terms (we do this because the concentration of primary radicals is significantly smaller than the concentration of the growing chains), and assume a one-dimensional traveling wave solution, *i.e.*, solutions that depend on $x = \xi_1 + ut$ where $u$ is the velocity of the reaction wave, we reduce the Equations (3) and (4) to

$$uJ' + \frac{1}{2}k_d J = 0, \tag{5a}$$

$$uM_1' + k_{\text{eff}1}\sqrt{\rho}JM_1H(J_0 - J) = 0, \tag{5b}$$

$$uM_2' + k_{\text{eff}2}\sqrt{1-\rho}JM_2H(J_0 - J) = 0, \tag{5c}$$

$$\frac{\kappa}{u}T'' = T' + q_1M_1' + q_2M_2'. \tag{6}$$

In these equations the prime denotes the derivative with respect to $x$ and $k_{\text{eff}j} = k_{pj}\sqrt{k_d/k_{tj}}$. We also introduce the Heaviside function $H$ into the equations to account for the inaccuracy of the steady-state approximation which allows polymerization reactions to occur prior to decomposition, a behavior which is inconsistent with the polymerization kinetics. The Heaviside functions is defined as

$$H(J_0 - J) = \begin{cases} 0, & J \geq J_0 \\ 1, & J < J_0 \end{cases},$$

so that polymerization cannot start if $J = J_0 \equiv \sqrt{I_0}$, *i.e.* if decomposition of the initiator has not started.

The boundary conditions associated with Equations (5), (6) are as follows. Far ahead of the wave ($x \to -\infty$) the conditions are the initial concentrations of initiator ($J_0$) and monomer ($M_{10}$,$M_{20}$) and the initial temperature ($T_0$):

$$J = J_0, \quad M_1 = M_{10}, \quad M_2 = M_{20}, \quad T = T_0. \tag{7}$$

Behind the wave ($x \to +\infty$)

$$T' = 0. \tag{8}$$

We can further simplify (6) by integrating the equation once and applying the boundary conditions (7) to get

$$\frac{\kappa}{u} T' = T - T_0 + q_1(M_1 - M_{10}) + q_2(M_2 - M_{20}). \tag{9}$$

Analysis of Equations (5) and (9) shows that in the limit $x \to +\infty$, $J$, $M_1$, $M_2$, and $T$ approach constant values. In particular, all of the initiator is consumed so $J$ goes to zero. However, the monomer concentrations do not necessarily vanish, so we denote these constants as $M_{1B}$ and $M_{2B}$. Using boundary condition (8) and Equation (9) we can express the temperature in the limit $x \to +\infty$ in terms of the final monomer concentrations as

$$T_B = T_0 + q_1(M_{10} - M_{1B}) + q_2(M_{20} - M_{2B}). \tag{10}$$

The values $M_{1B}$, $M_{2B}$ and $T_B$ along with the wave velocity $u$ are unknown. In the next section we determine these values because they give insight into the frontal polymerization process.

## 3. Solution procedure

In this section we study Equations (5) and (9) to determine the characteristics of the front. We use methods from combustion theory and perturbation techniques to obtain approximate solutions.

In combustion theory, nondimensional parameters, such as $R_g T_B / E_d$, determine the structure of the wave. Exploiting the fact that these parameters are small, one can replace the temperature-dependent, Arrhenius reaction rate constants with a simpler function where the integral of this new function over the temperature domain is approximately the same as the original function and the maximum height of the two functions are equal. Employing this technique leads to approximate analytic solutions known to be very accurate. Though frontal polymerization is much slower and significantly less exothermic than combustion processes, parameters of this form also determine the wave structure for frontal polymerization and happen to be small. Therefore, this technique can been used to determine approximate solutions for frontal polymerization. In fact, it has been used to study FP problems yielding accurate results [24, 27, 37, 38].

The simpler function with which we replace the kinetic parameter $k_\alpha(T)$ is the following step function

$$\hat{k}_\alpha(T) = \begin{cases} 0, & T < T_\alpha^{\text{ig}} \\ k_\alpha(T_B), & T > T_\alpha^{\text{ig}} \end{cases}, \tag{11}$$

where

$$T_\alpha^{\text{ig}} = T_B(1 - \epsilon_\alpha), \quad \epsilon_\alpha = R_g T_B / E_\alpha. \tag{12}$$

Here, again, $k_\alpha(T)$ is any Arrhenius exponential in the model, *i.e.*, the subscript $\alpha$ can be $p1$, $p2$, $t2$ and so on, and $\epsilon_\alpha$ is a small dimensionless parameter. The temperature $T_\alpha^{\text{ig}}$ is the temperature at which the corresponding reaction begins. Equation (12) accounts for the fact

that for large activation energies, ignition occurs within $O(\epsilon_\alpha)$ of the final burned temperature. Because of the presence of the Heaviside functions in the equations and due to the fact that the decomposition reaction activation energy $E_d$ is typically much larger than the other activation energies in the problem, all the reactions will begin simultaneously at the temperature $T_* = T_d^{\text{ig}}$, the temperature at which the decomposition reaction begins. Similar to combustion theory, the height of the chosen step function is equal to the maximum of the Arrhenius, temperature-dependent function and, the integral values of the two functions over the range $T_0$ to $T_B$ are approximately equal, which can be seen by approximately evaluating the integral

$$\int_{T_0}^{T_B} k_\alpha(T)\ \mathrm{d}T$$

using the Laplace method.

By replacing the reaction rate constants with step functions, we can consider Equations (5) and (9) in two regions: one where no reaction occurs and the other where all of the reactions occur. While we know the temperature at which the reactions begin, $T = T_*$, we need to determine the spatial point at which they begin. Since our equations are invariant under spatial translation, we can choose any point. For convenience, we define this point to be $x = 0$. Then, the equations ahead of the reaction front ($x < 0$) become

$$uJ' = 0, \quad uM_1' = 0, \quad uM_2' = 0, \tag{13a}$$

$$\frac{\kappa}{u}T' = T - T_0 + q_1(M_1 - M_{10}) + q_2(M_2 - M_{20})$$

with boundary conditions (7). The solution for this system is easily determined,

$$J(x) = J_0, \quad M_1(x) = M_{10}, \quad M_2(x) = M_{20}, \tag{14a}$$

$$T(x) = T_0 + (T_* - T_0)\exp\frac{u}{\kappa}x. \tag{14b}$$

In the region $x > 0$, the equations take the form

$$uJ' + \frac{1}{2}k_d^a J = 0, \tag{15a}$$

$$uM_1' + k_{\text{eff1}}^a\sqrt{\rho^a}\,JM_1 = 0, \tag{15b}$$

$$uM_2' + k_{\text{eff2}}^a\sqrt{1-\rho^a}\,JM_2 = 0, \tag{15c}$$

$$\frac{\kappa}{u}T' = T - T_0 + q_1(M_1 - M_{10}) + q_2(M_2 - M_{20}). \tag{15d}$$

In all of our equations, the superscript $a$ denotes that the quantity is evaluated at $T = T_B$.

At $x = 0$ we impose the boundary condition

$$J(0) = J_0, \quad M_1(0) = M_{10}, \quad M_2(0) = M_{20}, \quad \text{and} \quad T(0) = T_* \tag{16}$$

to ensure continuity of the solution. The boundary condition as $x \to \infty$ is given by Equation (8).

We now proceed to solve Equation (15). We define $A = M_1/M_2$ and divide Equations (15b) and (15c). This results in

$$\frac{\mathrm{d}M_1}{\mathrm{d}M_2} = k_r^a A^{3/2}, \tag{17}$$

where

$$k_r^a = (K_p^a)^{3/2}\left(\frac{k_{t1}^a}{k_{t2}^a}\right)^{-1/2}.$$

Since

$$\frac{\mathrm{d}M_1}{\mathrm{d}M_2} = M_2\frac{\mathrm{d}A}{\mathrm{d}M_2} + A,$$

we can rewrite (17) as

$$M_2\frac{\mathrm{d}A}{\mathrm{d}M_2} = k_r^a A^{3/2} - A \tag{18}$$

and solve to find the following equations for $M_1$ and $M_2$:

$$M_1(A) = M_{10}\frac{(k_r^a\sqrt{A}-1)^2}{(k_r^a\sqrt{A_0}-1)^2} \tag{19a}$$

$$M_2(A) = M_{20}\frac{A_0}{A}\frac{(k_r^a\sqrt{A}-1)^2}{(k_r^a\sqrt{A_0}-1)^2}. \tag{19b}$$

Next, we solve for the initiator concentration in terms of $A$. First we combine Equations (15a), (15c) and (18) to obtain

$$\frac{\mathrm{d}J}{\mathrm{d}A} = \frac{k_d^a}{2k_{\mathrm{eff2}}^a}\frac{\sqrt{K_p^a A+1}}{k_r^a A^{3/2}-A}. \tag{20}$$

Then we integrate Equation (20) to get

$$\frac{2k_{\mathrm{eff2}}^a}{k_d^a}(J(A)-J_0) = \int_{A_0}^{A}\frac{\sqrt{K_p^a\nu+1}}{k_r^a\nu^{3/2}-\nu}\mathrm{d}\nu. \tag{21}$$

If we let $x \to \infty$ in Equation (21), we obtain a condition for $A_B$

$$\frac{-2k_{\mathrm{eff2}}^a J_0}{k_d^a} = \int_{A_0}^{A_B}\frac{\sqrt{K_p^a\nu+1}}{k_r^a\nu^{3/2}-\nu}\mathrm{d}\nu. \tag{22}$$

Likewise, if we let $x \to \infty$ in Equations (19), then $A \to A_B$ and

$$M_{1B} = M_1(A_B) \quad \text{and} \quad M_{2B} = M_2(A_B). \tag{23}$$

These conditions and Equation (10) give us a closed system of equations for the unknown quantities $A_B$, $M_{1B}$, $M_{2B}$ and $T_B$.

Though the integrals in (21), (22) can be computed exactly, the resulting expressions are cumbersome. Since we desire simplified expressions for the unknown quantities, we compute

the integrals approximately. The assumption $|A_0 - A_B|/A_0 \ll 1$, which comes from an analysis of Equation (22) and the realization that the quantity $(2k^a_{\text{eff2}}J_0)/k^a_d$ is typically small, allows us to derive the following linear approximations for $J(A)$ and $A_B$:

$$J(A) = J_0 + (A - A_0)\frac{k^a_d}{2k^a_{\text{eff2}}}\frac{\sqrt{K^a_p A_0 + 1}}{k^a_r A_0^{3/2} - A_0} \tag{24}$$

and

$$A_B = A_0 - \frac{2k^a_{\text{eff2}}J_0(k^a_r A_0^{3/2} - A_0)}{k^a_d\sqrt{K^a_p A_0 + 1}}. \tag{25}$$

We can then substitute $A_B$ in Equations (23) and (10) to get expressions for $M_{1B}$, $M_{2B}$ and $T_B$.

We derive the equation to determine the velocity of the front by dividing Equation (15d) by (15a) and multiplying by Equation (20):

$$\frac{u^2}{\kappa}((T - T_0) + q_1(M_1(A) - M_{10}) + q_2(M_2(A) - M_{20}))\frac{J'(A)\mathrm{d}A}{J(A)} = -\frac{1}{2}k^a_d\mathrm{d}T. \tag{26}$$

We then note that in the reaction zone

$$T_B(1 - \epsilon_d) < T < T_B, \quad \epsilon_d \ll 1.$$

Since we are considering Equation (26) in the reaction zone and $\epsilon_d$ is small, we can replace $T$ with $T_B$ to rewrite Equation (26) as

$$\frac{u^2}{\kappa}\left[q_1(M_1(A) - M_{1B}) + q_2(M_2(A) - M_{2B})\right]\frac{J'(A)\mathrm{d}A}{J(A)} = -\frac{1}{2}k^a_d\mathrm{d}T. \tag{27}$$

Finally, we integrate both sides across the reaction zone to derive the integral expression for $u^2$,

$$u^2 = \frac{-\kappa k_d(T_B)}{2I_A}\frac{R_g T_B^2}{E_d} \tag{28}$$

where

$$I_A = \int_{A_0}^{A_B}\frac{J'(A)}{J(A)}\left(q_1(M_1(A) - M_{1B}) + q_2(M_2(A) - M_{2B})\right)\mathrm{d}A.$$

We can further simplify the expression for the velocity by Taylor expanding $I_A$ about $A_0$ to obtain

$$u^2 = \frac{\kappa J_0 k_d(T_B)}{2J'(A_0)(A_0 - A_B)}\frac{R_g T_B^2}{E_d(T_B - T_0)}. \tag{29}$$

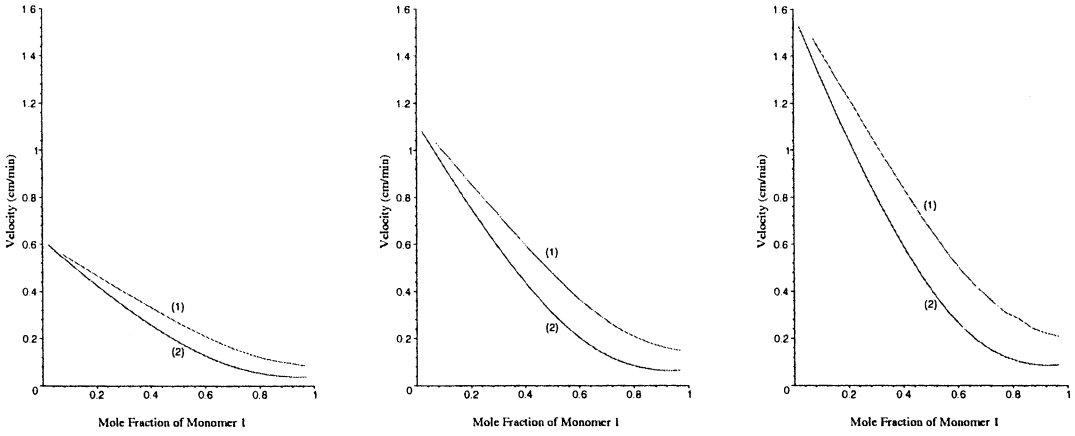


a. $J_0 = 0.1$ b. $J_0 = 0.2$ c. $J_0 = 0.3$

*Figure 1.* Velocity profiles for increasing initiator concentrations.Curve (1) – Numerical solution, curve (2) – Analytic approximation.

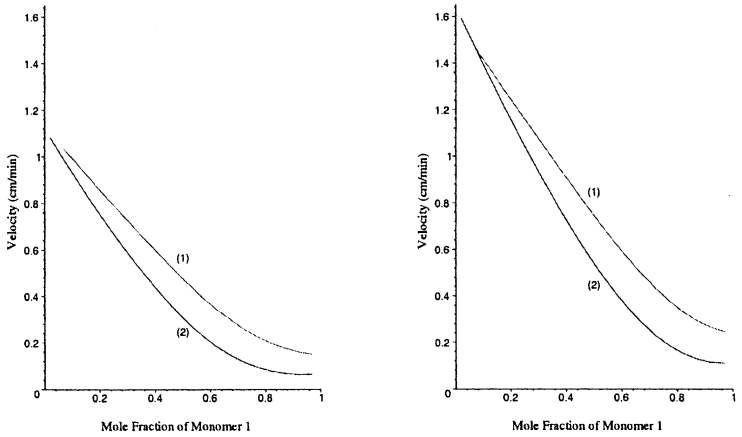


a. $T_0 = 303K$ b. $T_0 = 335K$

*Figure 2.* Velocity profiles for increasing initial temperature. Curve (1) – Numerical solution, curve (2) – Analytic approximation.

## 4. Results and discussion

The analytic solutions for the velocity and final monomer concentrations derived above allow us to examine which of the many parameters in our equations affect the velocity and temperature of the front, $T_B$. Though it is possible to solve the transcendental equation for $T_B$ approximately, we rely on an equation solver in MAPLE to extract this information. We compute numerical solutions to the original equations using a fourth order Runge-Kutta method with shooting on the velocity variable [39] and compare them to the analytical solutions. The parameters found in Tables 1 and **??** are used as base values for discussion and are typical values for free-radical polymerization [40]. The total concentration of the initial monomer is fixed at 12 mol/L, i.e. $M_{10} + M_{20} = 12$.

In frontal homopolymerization, the velocity of the front increases as the initiator concentration and the initial temperature increase [24]. We can see from Equation (29) that this should

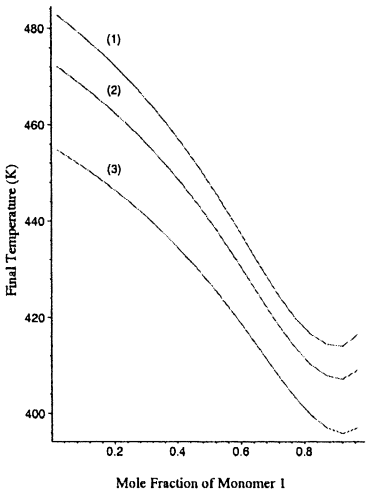


*Figure 3.* Front temperature for increasing initiator concentrations. Curve (1) – $J_0 = 0{\cdot}3$, curve (2) – $J_0 = 0{\cdot}2$, curve (3) – $J_0 = 0{\cdot}1$.

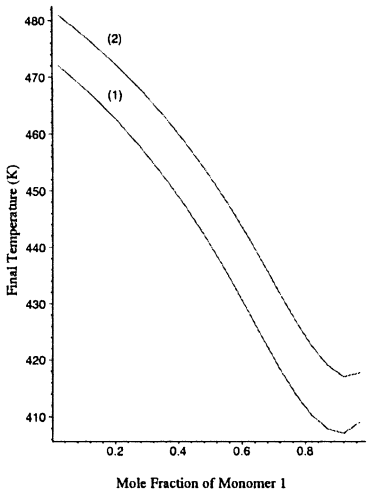


*Figure 4.* Front temperature for increasing initial temperature. Curve (1) – $T_0 = 303$ K, curve (2) – $T_0 = 335$ K.

*Table 1* Initiator and temperature parameters.

| Parameter | Value |
|---|---|
| $J_0$ (mol/L)$^{0{\cdot}5}$ | $0{\cdot}2$ |
| $k_d^0$ (1/s) | $2{\cdot}6 \times 10^{17}$ |
| $E_d$ (Cal/mol) | 29600 |
| $T_0$ (K) | 303 |
| $\kappa$ (cm$^2$/s) | $1{\cdot}42 \times 10^{-3}$ |

*Table 2* Kinetic parameters for monomers.

| | Monomer 1 | Monomer 2 |
|---|---|---|
| $k_p^0$ (L/mol · s) | $1{\cdot}8 \times 10^5$ | $4{\cdot}92 \times 10^6$ |
| $E_p$ (Cal/mol) | 1381 | 2530 |
| $k_t^0$ (L/mol · s) | $2{\cdot}21 \times 10^7$ | $9{\cdot}8 \times 10^6$ |
| $E_t$ (Cal/mol) | 250 | 700 |
| $q$ (L/K · m) | 30 | 33 |

also hold true in binary frontal polymerization. Figures 1 and 2, plots for starting initiator concentrations of $J_0 = 0{\cdot}1$, $0{\cdot}2$, and $0{\cdot}3$ and initial temperatures of $T_0 = 303$ K and $T_0 = 335$ K, respectively, confirm this relationship. These figures also verify a qualitative agreement between the analytic approximation and the full numerical solution of (5), (6).

Like velocity, $T_B$ increases as both the initiator concentration and initial temperature increase, see Figures 3 and 4. (We remark that Figures 3–8 are based on the approximate analysis). However, when we compare Figures 3 and 4 to velocity Figures 1 and 2, we find that the influence of $T_B$ on the velocity is not as we would expect. In homopolymerization and in copolymerization, the front temperature plays a dominant role in determining the velocity of the front. However, this is not the case in binary frontal polymerization as we will demonstrate.

In Figures 3 and 4, there is a clear minimum $T_B$ which occurs close to pure $M_1$. Likewise, in Figures 1 and 2 there is minimum velocity but it is not as obvious and it occurs much closer to pure $M_1$. We also observe that there is a change in concavity in temperature profiles, which does not occur in the velocity profiles. If $T_B$ were the dominant parameter in determining the velocity, the minimum $T_B$ and minimum velocity would occur at or near the same point and the rates of change in $T_B$ and velocity would be in agreement. Since this is not the case, we conclude that other factors are more influential in determining the velocity of the front.

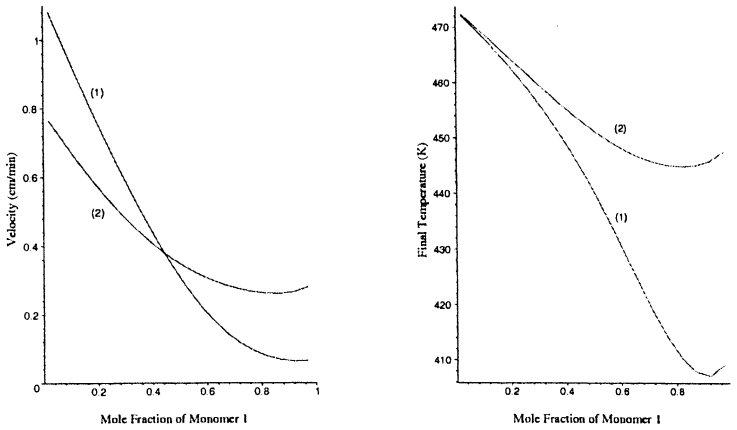


a. Front velocity b. Front temperature

*Figure 5.* Front velocity and temperature for increasing $k_{p1}^0$. Curve (1) – $k_{p1}^0 = 1{\cdot}8 \times 10^5$ (L/mol · s), curve (2) – $k_{p1}^0 = 7{\cdot}5 \times 10^5$ (L/mol · s).

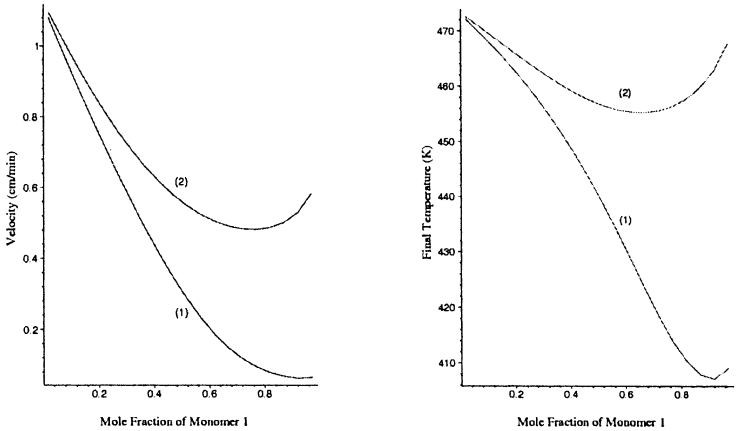


a. Front velocity b. Front temperature

*Figure 6.* Front velocity and temperature for decreasing $k_{t1}^0$. Curve (1) – $k_{t1}^0 = 2{\cdot}21 \times 10^7$ (L/mol · s), curve (2) – $k_{t1}^0 = 2{\cdot}21 \times 10^5$ (L/mol · s).

We will show that in BFP the kinetic parameters of the monomer and initiator have a greater influence on the velocity than the front temperature.

In our choice of kinetic parameters of the monomers, $k_{p1}^0$, the propagation frequency factor for $M_1$, is smaller than $k_{p2}^0$, the propagation frequency factor for $M_2$ and $k_{t1}^0$, the termination frequency factor for $M_1$, is larger than $k_{t2}^0$, the termination frequency factor for $M_2$. These two conditions imply that polymer chains ending in $M_2^*$ are more reactive and will remain reactive for a longer amount of time than chains ending in $M_1^*$. Because the frequency of the reactions for $M_2$ is larger, the velocity is faster for a higher concentration of $M_2$, as seen in Figures 1 and 2. If we increase the reactivity of $M_1$ by increasing $k_{p1}^0$, we see in Figure 5a that the velocity decreases for lower concentrations of $M_{10}$ and increases for higher concentrations of $M_{10}$. However, in Figure 5b we see that for all concentrations of $M_{10}$ the front temperature

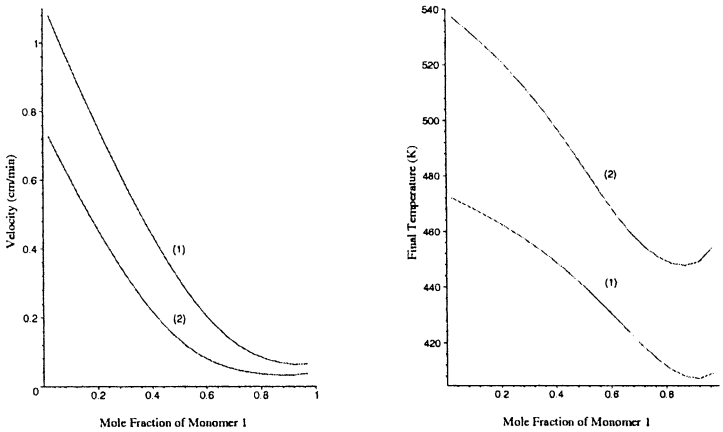


a. Front velocity b. Front temperature

*Figure 7.* Front velocity and temperature for decreasing $k_d^0$. Curve (1) – $k_d^0 = 2{\cdot}7 \times 10^{17}$ (1/s); $E_d = 29600$ (Cal/mol), curve (2) – $k_d^0 = 2{\cdot}7 \times 10^{15}$ (1/s); $E_d = 29600$ (Cal/mol).

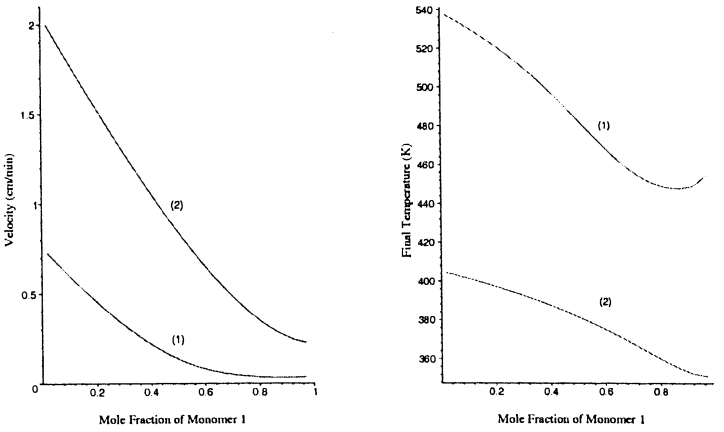


a. Front velocity b. Front temperature

*Figure 8.* Front velocity and temperature for decreasing $E_d$. Curve (1) – $k_d^0 = 2{\cdot}7 \times 10^{15}$ (1/s); $E_d = 29600$ (Cal/mol), curve (2) – $k_d^0 = 2{\cdot}7 \times 10^{15}$ (1/s); $E_d = 21000$ (Cal/mol).

increases for a larger $k_{p1}^0$. If $T_B$ were the most significant factor in determining the velocity, the relationship between the temperature and velocity would have been similar.

If we lower $k_{t1}^0$, we increase the ability of $M_1$ to react. This increases both the velocity of the front and the temperature of the front for all concentrations of $M_{10}$, as seen in Figure 6. We note that the location of the minimum $T_B$ and velocity are again not the same. Because Figures 5a and 6a show dramatic influences of the kinetic parameters on the velocity we deduce that the combination of the comonomer feed and the propagation and termination kinetics of the monomer are more important in determining the velocity of the front than the front temperature.

Next, we show that the initiator kinetics have an interesting influence on the front temperature and the velocity. Figures 7 and 8 show there is an inverse relationship between the

velocity and front temperature as we vary both the frequency factor and the activation energy of the initiator. If we decrease $k_d^0$, the velocity decreases and the front temperature increases, as can be seen in Figure 7. If $E_d$ is decreased, the velocity increases and the temperature decreases which is seen in Figure 8. Analyzing Equations (29) and (10), we can see that for this relationship to occur, $k_d^0$ must also be a controlling factor of the front velocity.

## 5. Conclusion

In this paper, we developed a model for binary frontal polymerization. Using simplifying assumptions, we derived expressions for final monomer concentrations, temperature at the front, and propagation velocity. These expressions were compared to numerical results of the full equation to demonstrate that the approximate analytical solutions are sufficiently accurate.

We also studied which parameters influence the velocity of the front. From our study, we conclude the comonomer feed and the kinetics of the monomers and initiator highly influence the front velocity, while the front temperature has less of an effect on the velocity. This is unusual since in frontal homopolymerization and frontal copolymerization the front temperature is dominant in determining the velocity of the front.

## Acknowledgements

This research has been supported in part by NSF grants DMS-0103856 and CTS-0138712.

## References

1. Y. Chekanov, D. Arrington, G. Brust and J.A. Pojman, Frontal curing of epoxy resin: Comparison of mechanical and thermal properties to batch cured materials. *J. Appl. Polym. Sci.* 66 (1997) 1209–1216.
2. A. Mariani, S. Fiori, Y. Chekanov and J.A. Pojman, Frontal ring-opening metathesis polymerization of dicyclopentadiene. *Macromolecules* 34 (2001) 6539–6541.
3. George Odian, *Principles of Polymerization.* New York: Wiley-Interscience (1981) 768 pp.
4. A. Rudin, *The Elements of Polymer Science and Engineering.* San Diego: Academic Press (1999) 509 pp.
5. J.A. Pojman, W. Elcan, A.M. Khan and L. Mathias, Binary polymerization fronts: A new method to produce simultaneous interpenetrating polymer networks (SINs). *J. Polym. Sci., Part A: Polym Chem.* 35 (1997) 227–230.
6. N.M. Chechilo, R.J. Khvilivitskii and N.S. Enikolopyan, On the phenomenon of polymerization reaction spreading. *Dokl. Akad. Nauk SSSR* 204 (1972) 1180–1181.
7. A.G. Merzhanov and I.P. Borovinskaya, New class of combustion processes. *Combust. Sci. Technol.* 10 (1975) 195–201.
8. N.M. Chechilo and N.S. Enikolopyan, Structure of the polymerization wave front and propagation mechanism of the polymerization reaction. *Dokl. Phys. Chem.* 214 (1974) 174–176.
9. N.M. Chechilo and N.S. Enikolopyan, Effect of the concentration and nature of initiators on the propagation process in polymerization. *Dokl. Phys. Chem.* 221 (1975) 392–394.
10. N.M. Chechilo and N.S. Enikolopyan, Effect of pressure and initial temperature of the reaction mixture during propagation of a polymerization reaction. *Dokl. Phys. Chem.* 230 (1976) 840–843.
11. J.A. Pojman, Traveling fronts of methacrylic acid polymerization. *J. Am. Chem. Soc.* 113 (1991) 6284–6286.
12. J.A. Pojman, J. Willis, D. Fortenberry, V. Ilyashenko and A. Khan, Factors affecting propagating fronts of addition polymerization: velocity, front curvature, temperature profile, conversion and molecular weight distribution. *J. Polym. Sci., Part A: Polym. Chem.* 33 (1995) 643–652.
13. J.A. Pojman, J.R. Willis, A.M. Khan and W.W. West, The true molecular weight distributions of acrylate polymers formed in propagating fronts. *J. Polym. Sci., Part A: Polym. Chem.* 34 (1996) 991–995.
14. A.M. Khan and J.A. Pojman, The use of frontal polymerization in polymer synthesis. *Trends in Polym. Sci.* 4 (1996) 253–257.

15. J.A. Pojman, I.P. Nagy and C. Salter, Traveling fronts of addition polymerization with a solid monomer. *J. Am. Chem. Soc.* 115 (1993) 11044–11045.
16. V.V. Barelko, A.D. Pomogailo, G.I. Dzhardimalieva, S.I. Evstratova, A.S. Rozenberg and I.E. Uflyand, The autowave modes of solid phase polymerization of metal-containing monomers in two- and three-dimensional fiberglass-filled matrices. *Chaos* 9 (1999) 342–347.
17. J.A. Pojman, G. Gunn, C. Patterson, J. Owens and C. Simmons, Frontal dispersion polymerization. *J. Phys. Chem. B* 102 (1998) 3927–3929.
18. J.A. Pojman, G. Curtis and V.M. Ilyashenko, Frontal polymerization in solution. *J. Am. Chem. Soc.* 115 (1996) 3783–3784.
19. Y.A. Chekanov and J.A. Pojman, Preparation of functionally gradient materials via frontal polymerization. *J. Appl. Polym. Sci.* 78 (2000) 2398–2404.
20. R.P. Washington and O. Steinbock, Frontal polymerization synthesis of temperature-sensitive hydrogels. *J. Am. Chem. Soc.* 123 (2001) 7933–7934.
21. I.P. Nagy, L. Sike and J.A. Pojman, Thermochromic composite prepared via a propagating polymerization front. *J. Am. Chem. Soc.* 117 (1995) 3611–3616.
22. I.P. Nagy, L. Sike and J.A. Pojman, Thermochromic composites and propagating polymerization fronts. *Adv. Mat.* 7 (1995) 1038–1040.
23. J. Szalay, I.P. Nagy, I. Barkai and M. Zsuga, Conductive composites prepared via a propagating polymerization front. *Die Ang. Makr. Chem.* 236 (1996) 97–109.
24. P.M. Goldfeder, V.A. Volpert, V.M. Ilyashenko, A.M. Khan, J.A. Pojman and S.E. Solovyov, Mathematical modeling of free-radical polymerization fronts. *J. Phys. Chem. B* 101 (1997) 3474–3482.
25. M. Apostolo, A. Tredici, M. Morbidelli and A. Varma, Propagation velocity of the reaction front in addition polymerization systems. *J. Polym. Sci., Part A: Polym. Chem.* 35 (1997) 1047–1059.
26. A. Tredici, R. Pecchiini and M. Morbidelli, Self-propagating frontal copolymerization. *J. Polym. Sci., Part A: Polym. Chem.* 36 (1998) 1117–1126.
27. M.F. Perry, V.A. Volpert, L.L. Lewis, H.A. Nichols and J.A. Pojman, Free-radical frontal copolymerization: The dependence of the front velocity on the monomer feed composition and reactivity ratios. *Macromolecular Theory and Simulations* 12 (2003) 276–286.
28. G. Bowden, M. Garbey, V.M. Ilyashenko, J.A. Pojman, S. Solovyov, A. Taik and V. Volpert, The effect of convection on a propagating front with a solid product: Comparison of theory and experiments. *J. Phys. Chem. B* 101 (1997) 678–686.
29. B. McCaughey, J.A. Pojman, C. Simmons and V.A. Volpert, The effect of convection on a propagating front with a liquid product: comparison of theory and experiments. *Chaos* 8 (1998) 520–529.
30. J. Masere, F. Stewart, T. Meehan and J.A. Pojman, Period-doubling behavior in frontal polymerization of multifunctional acrylates. *Chaos* 9 (1999) 315–322.
31. V.M. Ilyashenko and J.A. Pojman, Single head spin modes in frontal polymerization. *Chaos* 8 (1998) 285–289.
32. J.A. Pojman, J. Masere, E. Petretto, M. Rustici, D.-S. Huh, M.S. Kim and V. Volpert, The effect of reactor geometry on frontal polymerization spin modes. *Chaos* 12 (2002) 56–65.
33. J.A. Pojman, V.M. Ilyashenko and A.M. Khan, Spin mode instabilities in propagating fronts of polymerization. *Physica D* 84 (1995) 260–268.
34. D.A. Schult and V.A. Volpert, Linear stability analysis of thermal free radical polymerization waves. *Int. J. Self-Propag. High-Temp. Synthesis* 8 (1999) 417–440.
35. C.A. Spade and V.A. Volpert, Linear stability analysis of non-adiabatic free-radical polymerization waves. *Combust. Theory Modell.* 5 (2001) 21–39.
36. L.K. Gross and V.A. Volpert, Weakly nonlinear stability analysis of frontal polymerization. *Stud. Appl. Math.* 110 (2003) 351–376.
37. C.A. Spade and V.A. Volpert, On the steady state approximation in thermal free radical frontal polymerization. *Chem. Engng. Sci.* 55 (2000) 641–654.
38. P.M. Goldfeder and V.A. Volpert, Nonadiabatic frontal polymerization. *J. Engng. Math.* 34 (1998) 301–318.
39. D. Kincaid and W. Cheney, *Numerical Analysis*. Pacific Grove, CA: Brooks/Cole Publishing Co. (2001) 804 pp.
40. J. Brandrup and E.H. Immergut, *Polymer Handbook*. New York: John Wiley and Sons (1999) 2336 pp.